Supplementary Information

Kinetically-Arrested Single-Polymer Nanostructures from Amphiphilic Mikto-Grafted Bottlebrushes in Solution: A Simulation Study

Bahar Gumus, Margarita Herrera-Alonso and Abelardo Ramirez-Hernandez

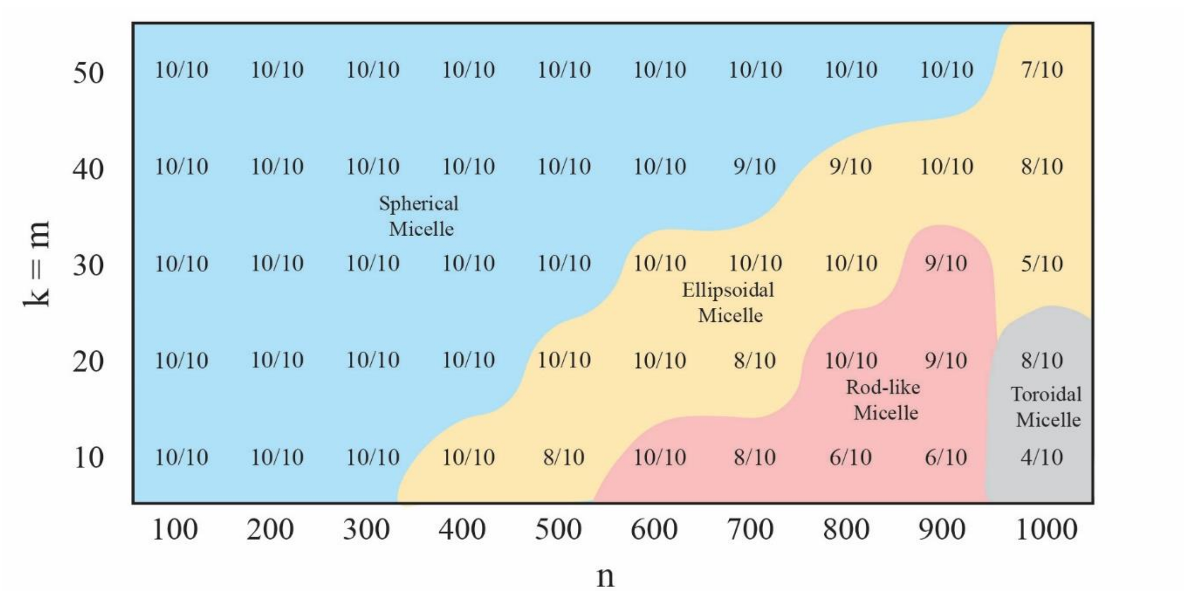

Figure S1. Morphology diagram of symmetric ($k = m$) molecular bottlebrushes (C-g-A_k/B_m)$_n$ in the parameter space (n,k) representing the number of macromonomers and side chains' degree of polymerization, respectively, for weak incompatibility ($a_{AB} = 30$). Each morphology represents the more frequent structure (of ten different initial configurations) that is obtained following the simulation protocol described in the Methods section on the main text. Numbers represent the number of times that a given morphology is obtained of the total of ten independent simulations.

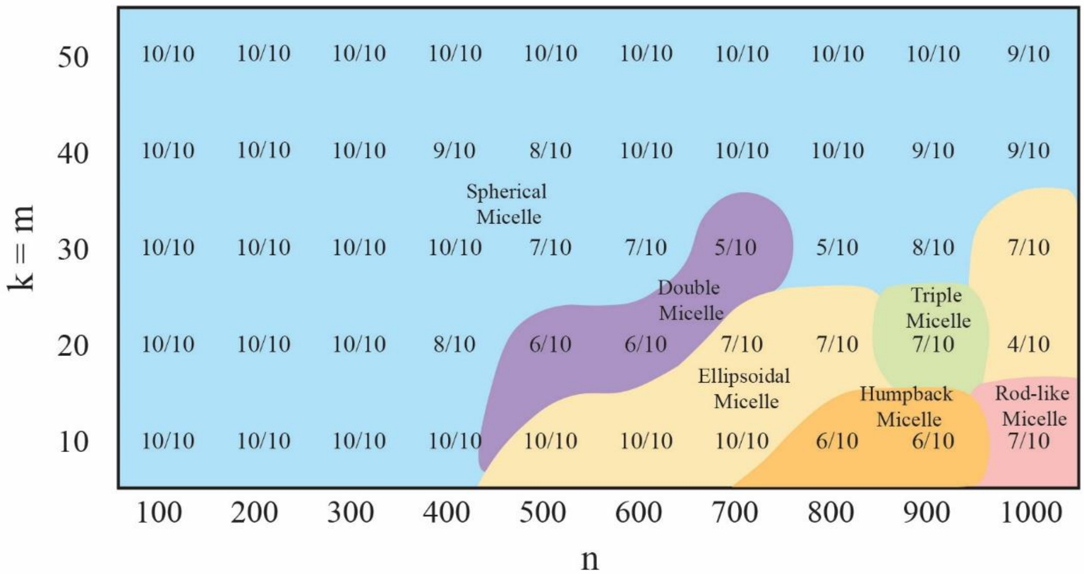

Figure S2. Morphology diagram of symmetric ($k = m$) molecular bottlebrushes (C-g-A_k/B_m)$_n$ in the parameter space (n,k) representing the number of macromonomers and side chains' degree of polymerization, respectively, for weak incompatibility ($a_{AB} = 70$). Each morphology represents the more frequent structure (of ten different initial configurations) that is obtained following the simulation protocol described in the Methods section on the main text. Numbers represent the number of times that a given morphology is obtained of the total of ten independent simulations.

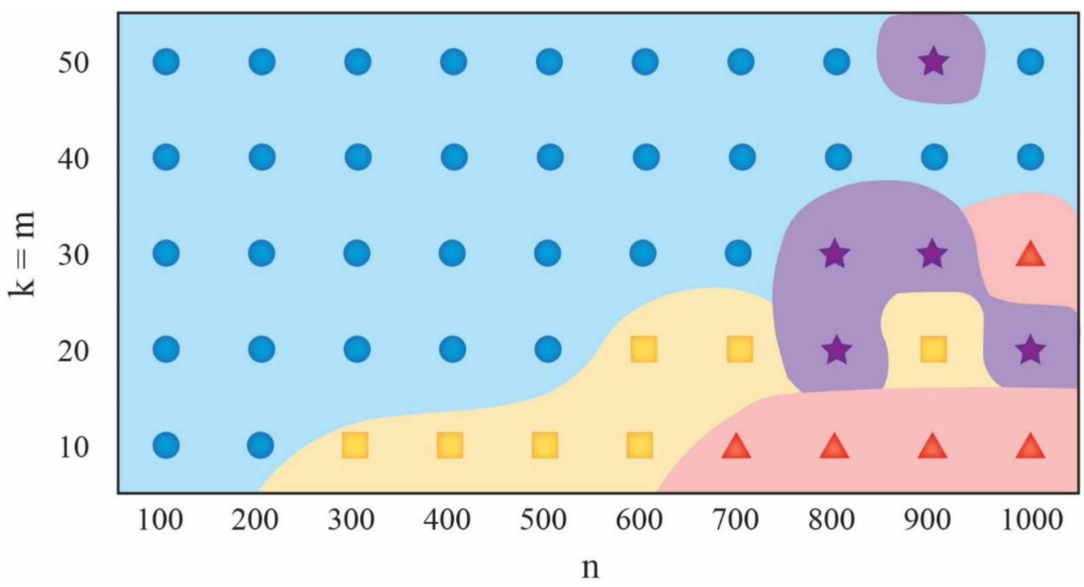

Figure S3.Morphology diagram of symmetric ($k = m$) molecular bottlebrushes (C-g-A_k/B_m)$_n$ in the parameter space (n,k) representing the number of macromonomers and side chains' degree of polymerization, respectively, for $a_{AB} = 50$. Only one initial configuration per point was used to build this diagram. Symbols are same as those in the diagrams on the main text.

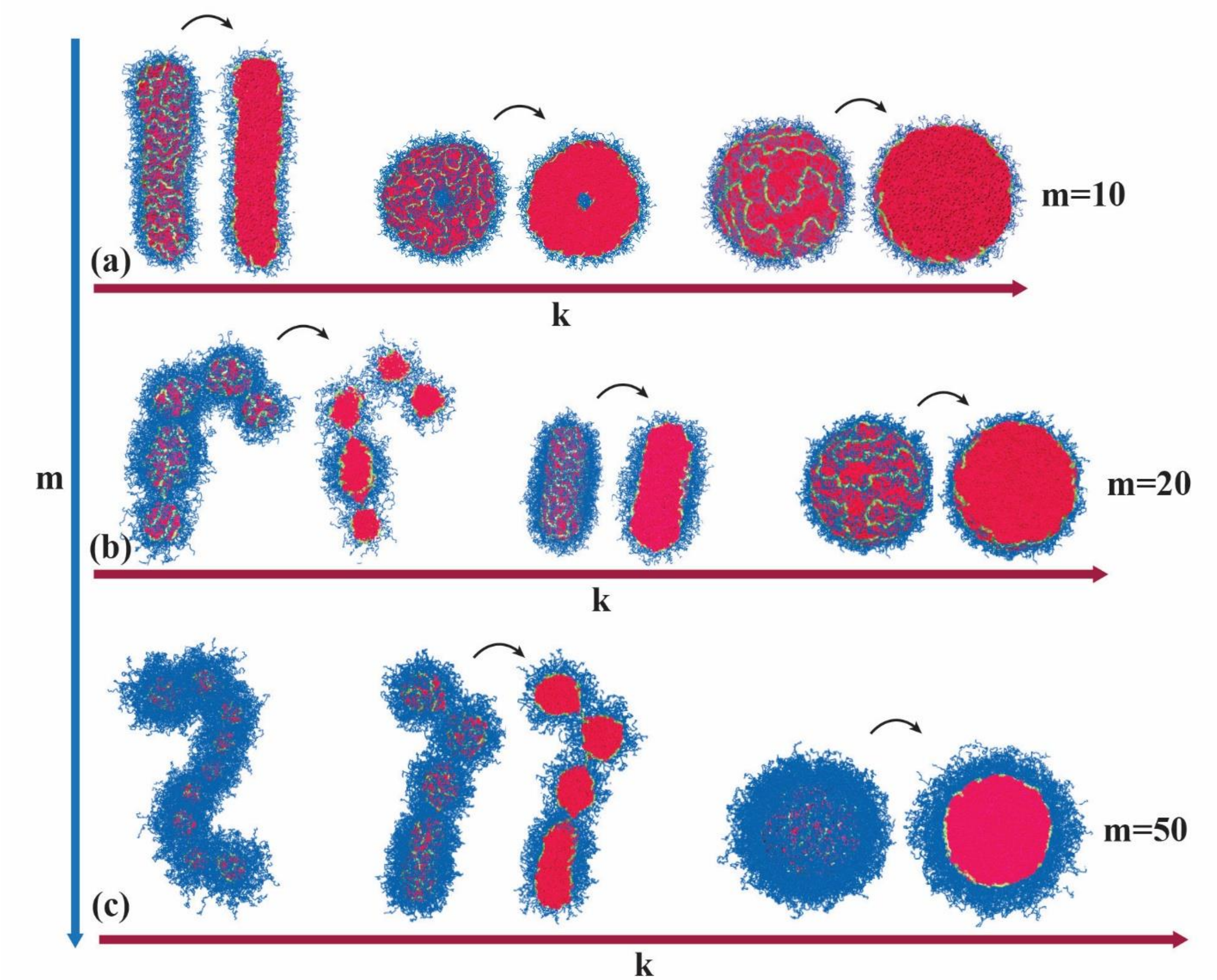

Figure S4. Representative single-polymer self-assembled nanostructures obtained after a fast quench into a bad solvent condition for one of the side chains (red domains), formed by $(C\text{-}g\text{-}A_k/B_m)_{1000}$ asymmetric bottlebrushes. Solvophilic side chains are displayed in blue, whereas the bottlebrush backbone is represented by the green tube wrapping around the solvophobic cores. Solvent molecules are not displayed for clarity. The solvophilic block molecular weight is fixed at (a) m=10, (b) m=20, and (c) m=50. Solvophobic side chain molecular weight, k, increases from left to right. The chemical incompatibility between A and B polymer segments was fixed at $at\ a_{AB} = 50$. Same morphologies as the ones presented in the main text (Figure 5), but we have added cross-section images.

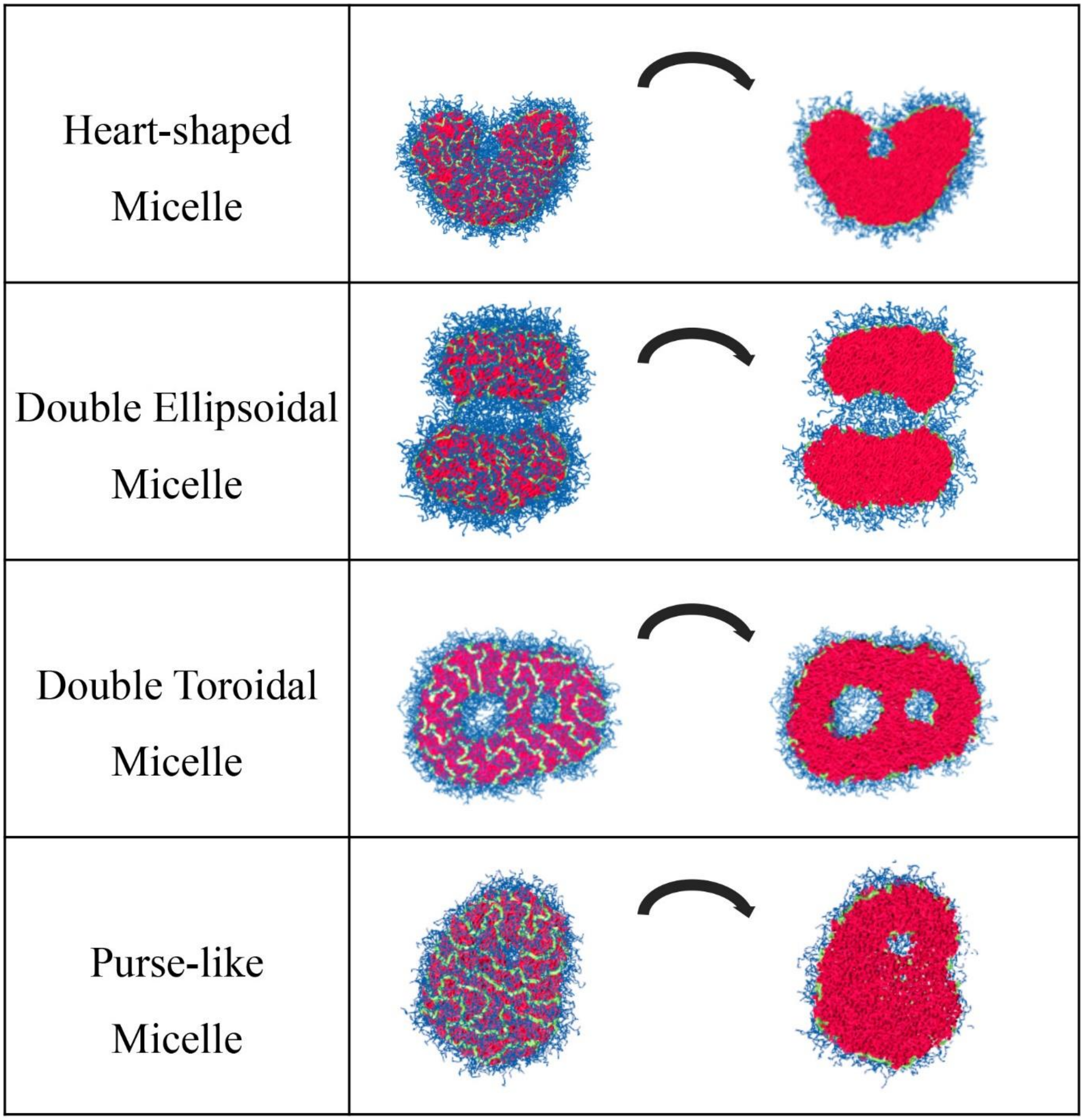

Figure S5. Single-polymer self-assembled nanostructures obtained after a fast quench into a bad solvent condition for one of the side chains (red domains). Although these are not the most frequent morphologies, they are part of the possible self-assembled nanostructures can that be obtained by the mikto-grafted bottlebrushes considered in this work. Solvophilic side chains are displayed in blue, whereas the bottlebrush backbone is represented by the green tube wrapping around the solvophobic cores. Solvent molecules are not displayed for clarity. Two snapshots are presented, the image on the right is a cross-section of the image on the left. Images are not at the same scale.

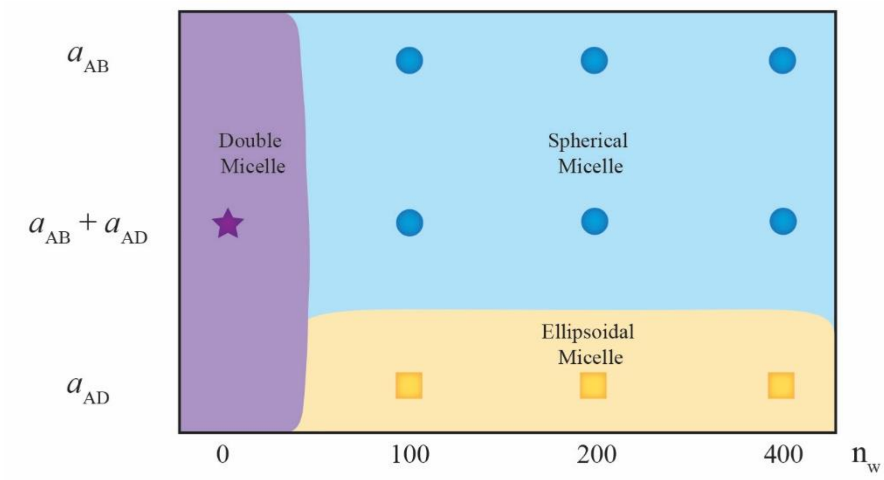

Figure S6. Self-assembled morphologies obtained by following different quenching protocols for a symmetric bottlebrush with $n = 600$ and $k = 20$. Simulations are divided into n_w stages, and at each stage the corresponding parameter(s) are increased by $\delta a_{ij} = (a_{ij}^f - a_{ij}^0)/n_w$, where a_{ij}^0=25 to a_{ij}^f=70. See main text for more details. Under an instantaneous quench ($n_w = 0$) a double-micelle structure is formed, however, by doing a slow quenching, the macromolecule self-assembled into a different morphology.

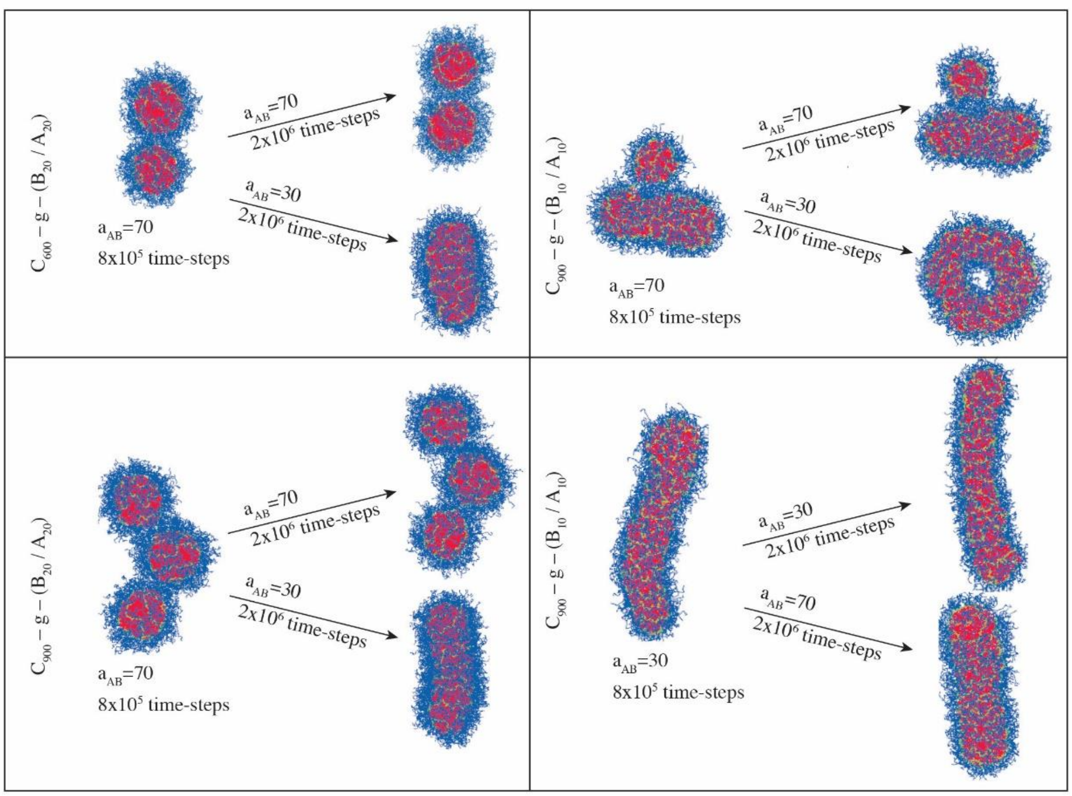

Figure S7. Effect of lower incompatibility between side chains on complex micelle structures. Self-assembled structures of symmetric bottlebrushes under a fast quench after 8×10^5 time steps were used as initial configurations for evolving another 2×10^6 time steps under same incompatibility values $a_{AB} = 70$ or under a lower incompatibility $a_{AB} = 30$. By decreasing the incompatibility, multi-micelles structures evolved toward single-micelle morphologies. However, when a single-micelle structure formed under low incompatibility is evolved at a higher incompatibility, the micelle does not form a multi-micelle (lower right figure).

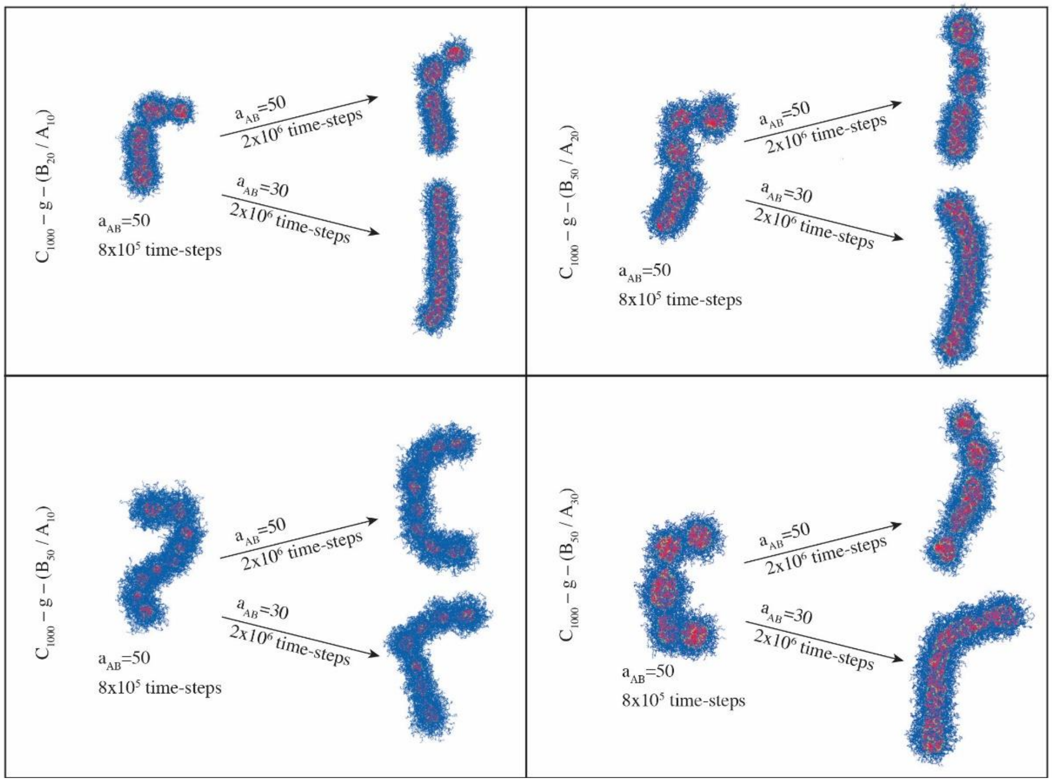

Figure S8. Effect of lower incompatibility between side chains on complex micelle structures. Self-assembled structures of asymmetric bottlebrushes under a fast quench after 8×10^5 time steps were used as initial configurations for evolving another 2×10^6 time steps under same incompatibility values $a_{AB} = 50$ or under a lower incompatibility $a_{AB} = 30$. By decreasing the incompatibility, most of the multi-micelles structures evolved toward single-micelle morphologies. The only case that did not completely transformed into a single-micelle is the one where the A side chain is 5 times smaller than B side chains. For this case, we suspect that the relative longer corona, protecting the hydrophobic cores, is making the evolution slower.

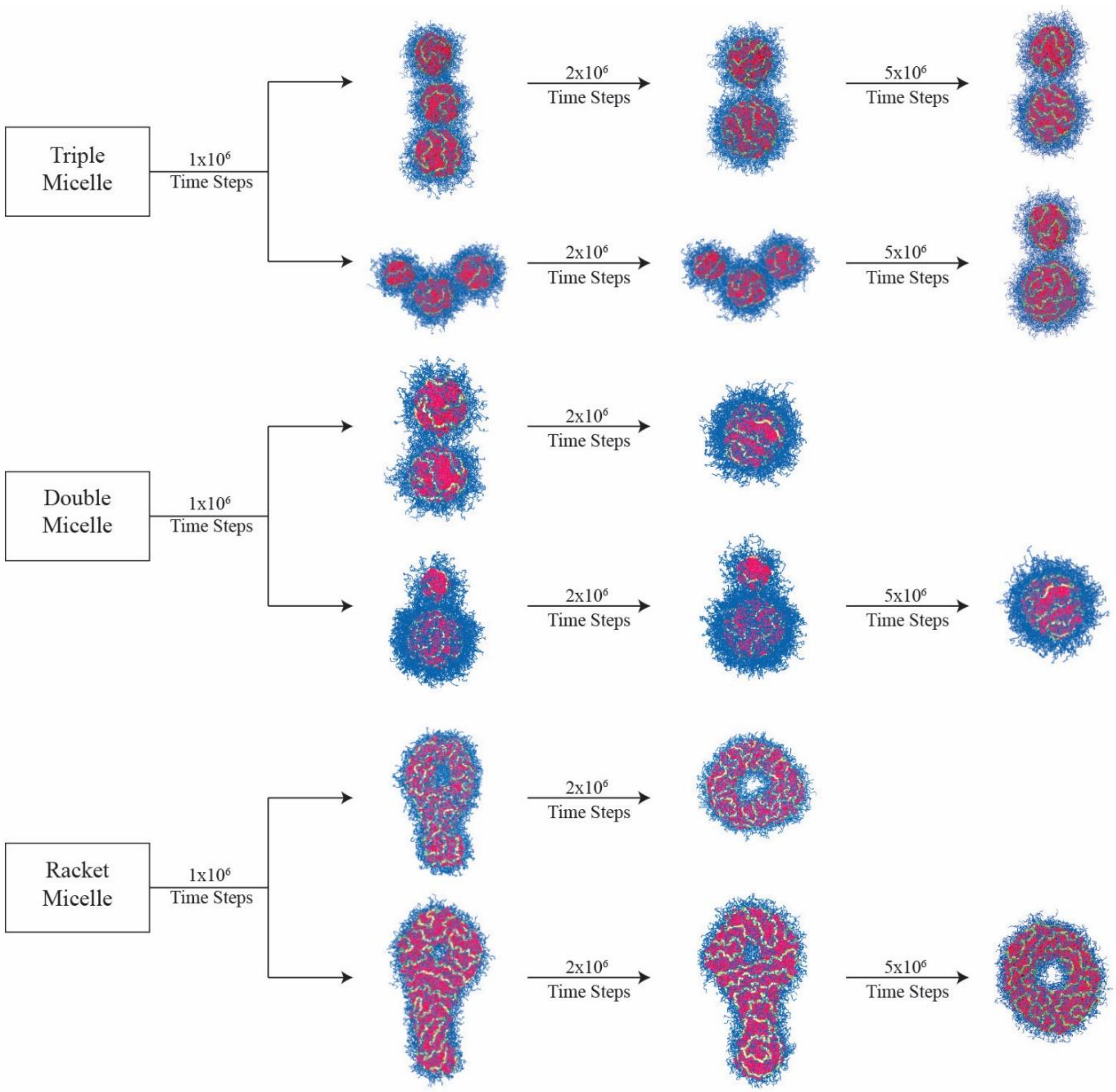

Figure S9. Self-assembled structures of symmetric mikto-grafted bottlebrushes obtained after a fast quench into a bad solvent condition. Ten different random initial configurations were run for 10^6 time steps. To check the stability of the obtained morphologies, selected systems were replicated three times and run for an additional 10^6 time steps. Few of those nanostructures evolved into a slightly different structure. In this Figure we present cases that evolved into a different morphology, and some that did not after those 10^6 time steps. Additional 3×10^6 time steps were simulated for those single realizations that seem to be still evolving. The symmetric bottlebrushes in the figure correspond to (from top to bottom): case (1) a_{AB}=70, n=900, k=20; (2) a_{AB}=70, n=500, k=20; (3) a_{AB}=30, n=1000, k=10.